

Review

In vivo clinical molecular imaging of T cell activityXiaju Cheng,^{1,3} Jiahao Shen,^{1,3} Jingwei Xu,^{2,*} Jinfeng Zhu,¹ Pei Xu,¹ Yong Wang,^{1,*} and Mingyuan Gao ^{1,4,*}

Tumor immunotherapy is refashioning traditional treatments in the clinic for certain tumors, especially by relying on the activation of T cells. However, the safety and effectiveness of many antitumor immunotherapeutic agents are suboptimal due to difficulties encountered in assessing T cell responses and adjusting treatment regimens accordingly. Here, we review advances in the clinical visualization of T cell activity *in vivo*, and focus particularly on molecular imaging probes and biomarkers of T cell activation. Current challenges and prospects are also discussed that aim to achieve a better strategy for real-time monitoring of T cell activity, predicting prognoses and responses to tumor immunotherapy, and assessing disease management.

Enhancing T cell function via immunotherapy

Tumor immunotherapies, such as **immune checkpoint blockade (ICB)** (see [Glossary](#)) [1] and **chimeric antigen receptor-T cell (CAR-T)** infusions [2], have been implemented in the clinical setting for cancer treatment. However, the complex tumor microenvironment (TME) and **intratumor heterogeneity (ITH)** pose significant obstacles to the survival and proliferation of immune cells, hindering the ability of the latter to effectively combat cancer [3]. Indeed, the clinical response rates of such therapies remain low. It is well known that T cells have a crucial role in the systemic immune response by recognizing tumor antigens and initiating tumor-specific immunity. However, the ‘Hellstrom paradox’ acknowledges the coexistence of T cells and cancer cells within the tumor, highlighted by a dysfunctional T cell response known as ‘T cell exhaustion’ [4]. In contrast to activated effector T cells, exhausted T cells express increased amounts of inhibitory receptors, such as programmed cell death-1 (PD-1) and cytotoxic T lymphocyte-associated antigen-4 (CTLA-4), and show reduced proliferation and cytotoxicity, as well as imbalanced redox homeostasis in T cells (Figure 1) [5,6]. However, long sought-after approaches have aimed to restore the effector function of early-stage dysfunctional T cells, such as by using ICB, or, from another angle, the stimulation of phosphoinositide 3-kinase (PI3K) and mitogen-activated protein kinase (MAPK) signaling pathways [7]; alternatively, increasing the expression of nuclear factors of activated T cells (NFAT) and activator protein 1 (AP-1) transcription factors has also been considered [8], among other approaches.

Personalization of tumor immunotherapies might help boost therapeutic efficacy if tumor responses to treatment can be assessed in a timely fashion. Currently, the evaluation of a patient’s response to immunotherapy may involve measuring the expression of immune checkpoint receptors in tumors and immune cells [e.g., PD-1, programmed cell death ligand 1 (PD-L1), etc.] [9], as well as the numbers of immune cells present in peripheral blood and tumors (e.g., cytotoxic CD8⁺ T cells) [10], in addition to associated symptoms. For instance, the number of tumor-infiltrating lymphocytes (TILs), such as CD3 [11,12] and CD8 [13,14], can be tracked using positron emission tomography (PET) in clinical settings. However, assessing the responsiveness of these immune cells against a tumor is challenging due to the complexity of the TME and immunosuppressive factors [15]. In this context, we argue that assessing T cell activity during antigen presentation, T cell antigen recognition, and co-stimulatory signaling might improve understanding of tumor responses to

Highlights

Immunotherapy has gained significant attention for its remarkable efficacy in combating tumors, such as in cases of immune checkpoint blockade and chimeric antigen receptor (CAR)-T treatments. However, the low response rate for certain tumors remains an outstanding challenge.

The therapeutic efficacy of immunotherapy based on stimulating immune activation largely relies on the cytotoxic antitumor activity of CD8⁺ T cells. However, tumor microenvironment complexity and heterogeneity, as well as heterogeneous and dynamic tumor-infiltrating T cells (including exhausted cells), create significant challenges for treating patients with cancer.

The accurate and comprehensive assessment of T cell activity *in vivo* via clinical molecular imaging techniques (along with other approaches) can better inform clinicians of tumor response predictions, ideally optimizing immunotherapy regimens.

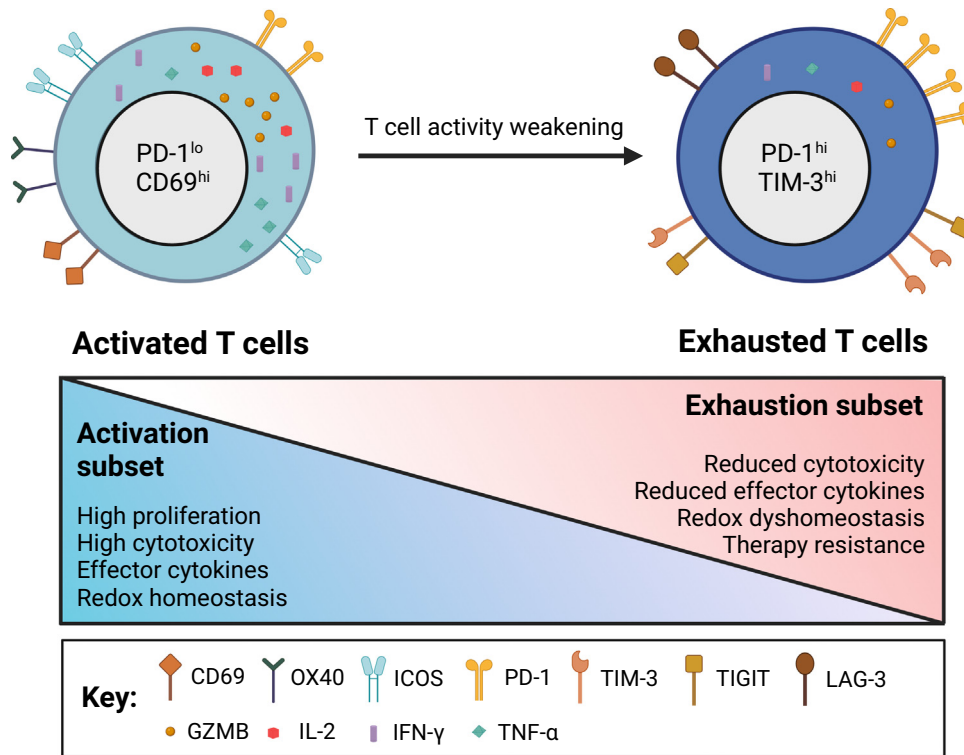
Recent advances in molecular imaging techniques for non-invasive and quantitative visualization of T cells *in vivo* through positron emission tomography, magnetic resonance imaging, and fluorescence imaging, among others, are further facilitating the assessment of antitumor activity.

Versatile targets, including metabolites, redox substances, surface receptors, and secreted cytokines, are emerging, in many cases proving to be suitable for monitoring T cell activity *in vivo*.

Significance

Tumor immunotherapies have yet to be optimized and real-time *in vivo* assessment of antitumor responses represents an important tool to monitor and improve therapeutic efficacy. Tumor-specific T cell immunity is hampered by T cell dysfunction. In this context, targeting molecular candidates





(e.g., surface receptors, secreted factors, and molecules that are relevant in metabolism and redox status) for real-time *in vivo* imaging of T cell activity may enable a better understanding of immunotherapy-mediated antitumor responses.

¹Key Laboratory of Radiation Medicine and Protection, School for Radiological and Interdisciplinary Sciences (RAD-X), Collaborative Innovation Center of Radiation Medicine of Jiangsu Higher Education Institutions, Soochow University, Suzhou 215123, PR China
²Department of Cardiothoracic Surgery, Suzhou Municipal Hospital Institution, Suzhou 215000, PR China
³These authors contributed equally
⁴Lead contact

*Correspondence: xujw110447@163.com (J. Xu), yongwang@suda.edu.cn (Y. Wang), and gaomy@suda.edu.cn (M. Gao).

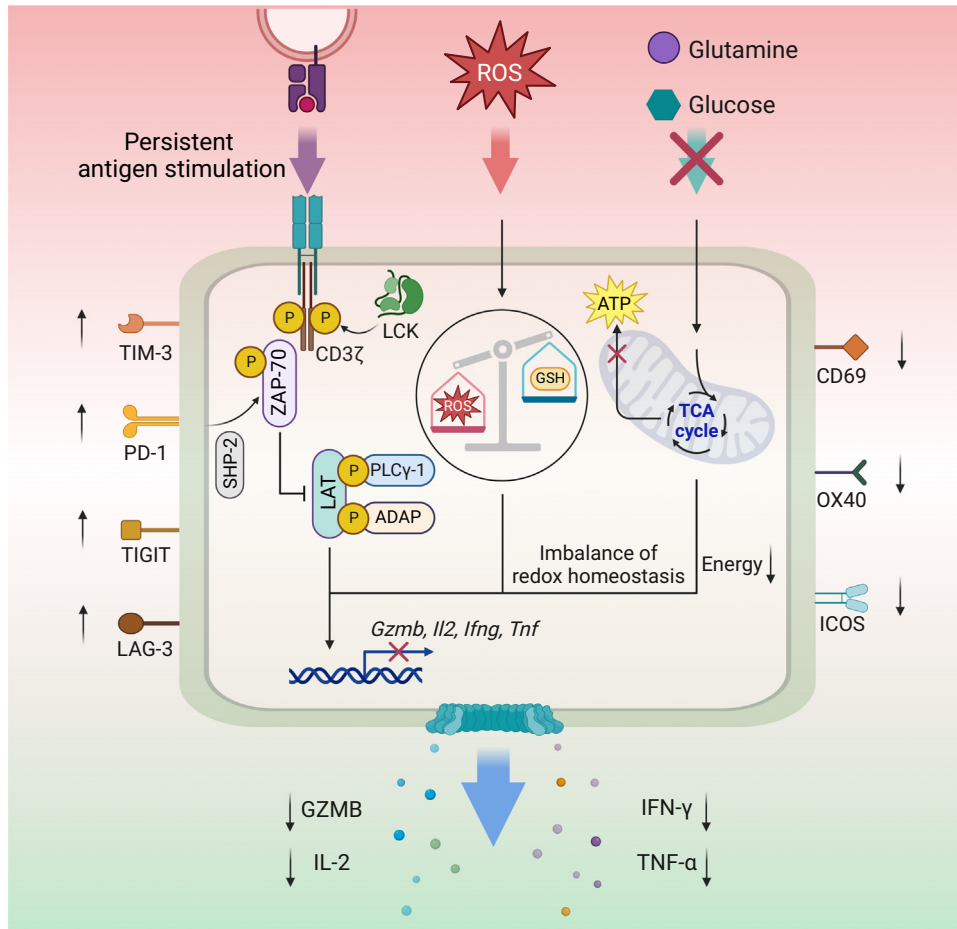
Trends in Immunology

Figure 1. Diverse phenotypes of activated T cells and exhausted CD8⁺ T cells. CD8⁺-activated T cells are characterized by the upregulated expression of various immune-activating receptors on the surface, such as CD69 and OX40, and high proliferation and cytotoxicity with the secretion of effector cytokines, as well as intracellular redox homeostasis. However, in the presence of cancer or chronic viral infections, T cell activity can weaken, leading to a state of exhaustion, which is associated with decreased proliferation, reduced production of effector cytokines, imbalance of redox homeostasis, and elevated expression of multiple inhibitory receptors (e.g., PD-1, etc.). Unfortunately, this subset of T cells may not respond well to immunotherapy. Abbreviations: GZMB, granzyme B; ICOS, inducible T cell co-stimulator; IFN, interferon; IL, interleukin; LAG-3, lymphocyte-activation gene 3; PD-1, programmed cell death-1; TIGIT, T cell immunoreceptor with Ig and ITIM domains; TIM-3, T cell immunoglobulin and mucin domain-3; TNF-α, tumor necrosis factor-α. Figure created using BioRender ([biorender.com](https://www.biorender.com)).

immunotherapy. One important consideration is that the status of T cell activity depends on various factors, such as intracellular metabolism and microenvironmental factors, including persistent antigen stimulation, excessive reactive oxygen species (ROS), and nutrient restriction; these can alter T cell receptor (TCR) signaling, epigenetic landscapes, redox homeostasis, surface receptor expression, effector cytokine secretion, and other molecular changes (Figure 2) [4]. We posit that molecular imaging tools are beginning to provide versatile innovative approaches for non-invasively assessing the efficacy of immunotherapies, many of which monitor certain known biomarkers associated with T cell activation. We do not focus here on the various molecular imaging techniques used in basic immunology, such as 2-photon microscopy, among others (Box 1). Instead, we summarize state-of-the-art progress in clinical molecular imaging techniques that are relevant for assessing T cell activation by monitoring metabolism, redox status, surface receptors, and secreted molecules in T cells, among others (Figure 3, Key figure). Innovations in, and challenges of, *in vivo* T cell visualization relative to tumor immunotherapy are also discussed.

Using molecular imaging to visualize T cell activity *in vivo*

Clinical molecular imaging integrates conventional medical imaging with molecular biology, enabling molecular probes to monitor certain physiological characteristics *in vivo* [16]. Established



Trends in Immunology

Figure 2. T cell activity depends on various external cues in the microenvironment as well as intracellular signal transduction. The antigen-presenting cells (APCs) present peptide-major histocompatibility complex (pMHC) to T cell receptors (TCRs) on T cells, activating downstream signaling transduction. However, persistent antigen stimulation can induce T cell exhaustion, downregulating immune-activating receptors, and upregulating immune-inhibitory receptors to inhibit TCR signaling pathway activation. Excessive reactive oxygen species (ROS) in the microenvironment can cause extracellular or intracellular imbalance of redox homeostasis in T cells. Additionally, tumor cells and immunosuppressive cells can limit the biosynthetic metabolism of T cells through nutrient restriction, decreasing the secretion of various effector cytokines, such as granzyme B (GZMB), interleukin (IL)-2, interferon (IFN)- γ , and tumor necrosis factor (TNF)- α . Abbreviations: ADAP, adhesion and degeneration-promoting adaptor protein; GSH, glutathione; *Ifng*, *interferon- γ gene*; *ICOS*, *inducible T cell co-stimulator*; *LAG-3*, *lymphocyte-activation gene 3*; SHP-2, Src homology-2 domain-containing protein tyrosine phosphatase-2; TCA, tricarboxylic acid; TIGIT, T cell immunoreceptor with Ig and ITIM domains; TIM-3, T cell immunoglobulin and mucin domain-3; ZAP-70, zeta-chain-associated protein kinase 70. Figure created using BioRender ([biorender.com](https://www.biorender.com)).

non-invasive imaging techniques, including PET, single photon emission computed tomography (SPECT), magnetic resonance imaging (MRI), fluorescence (FL) imaging and others, may allow the monitoring of immunomodulation *in vivo*. Examples of immune targets for visualizing T cell activity *in vivo* are summarized below (Table 1).

Metabolism-associated targets

Insufficient intracellular nutrient anabolism, such as glycogen, nucleotides, and amino acids, among others, largely contributes to T cell dysfunction [17]. Although T cell metabolism is widely assessed *via in vitro* assays, invasive and/or endpoint measurements, such as quantification of

Glossary

β -counting: radiocounting technique to measure radioactivity of a radionuclide by quantifying the β particles emitted during radioactive decay.

2-deoxy-2-(^{18}F)fluoro-D-glucose (^{18}F -FDG) PET imaging: imaging technique utilizing a glucose analog ^{18}F -FDG probe to visualize and assess metabolic processes in animals or humans through PET imaging; widely used for clinical cancer diagnosis due to the high energy requirements of cancer cells.

Chimeric antigen receptor T cell (CAR-T): engineered T cells constructed through a series of processes, including extracting T cells from the patient with cancer, and modifying them *in vitro* to express CARs. CAR-T cells are autologously infused back into the patient to recognize specific antigens on cancer cells.

Fluorescence resonance energy transfer (FRET): fluorescence imaging technique utilizing energy transfer from an excited donor molecule to a nearby acceptor molecule, resulting in a change in fluorescence intensity to image the interaction between two proteins or cells.

Hyperpolarized ^{13}C MRI: imaging technique utilizing a substance containing hyperpolarized ^{13}C to enhance the ^{13}C MRI signal through alignment of specific atoms; used in studies of metabolic processes.

Immune checkpoint blockade (ICB): immunotherapy using immune checkpoint inhibitor(s) to help reactivate CD8 $^{+}$ T cells to kill cancer cells (e.g., blocking the PD-1/PDL-1 signaling axis).

ImmunoPET: molecular imaging modality combining the superior targeting specificity of a monoclonal antibody and the inherent PET imaging sensitivity of radionuclides to detect immune cell subsets, activation/inhibitory biomarkers, and to track adoptively transferred cellular therapeutics, and so on.

Immunoreceptor tyrosine-based activation motifs (ITAMs): short amino acid sequences harboring the conserved Y_{xxLxV} motif; located in the cytoplasmic domains of various transmembrane proteins on immune cells; facilitate signal transduction of an extracellular activation signal to an intracellular one, enabling immune cell activation.

Intratumor heterogeneity: genetic and phenotypic diversity within a single tumor, indicating that different cells

Box 1. Examples of intracellular protein targets used *in vitro* for T cell imaging

APCs present peptide-major histocompatibility complex (pMHC) to the TCR on T cells, initiating intracellular downstream signal transduction involving a series of protein phosphorylation events [86]. Phosphorylation of **immunoreceptor tyrosine-based activation motifs (ITAMs)** in the cytoplasmic tails of TCR-CD3 by Lck or Fyn, recruits zeta-chain-associated protein kinase 70 (ZAP-70) to the TCR [87,88], which phosphorylates the **linker for activation of T cells (LAT)** to form the LAT signalosome, initiating T cell activation [89,90]. These sophisticated immune events offer an opportunity to design innovative probes for further monitoring the activation of T cells.

Visualizing protein clusters in living cells can be challenging but advanced single-molecule techniques utilizing optical microscopy have quantified protein clustering in the **T cell immune synapse (IS)**, enabling high spatial and temporal resolution evaluation of T cell activation [91,92]. For example, TIRFM and fluorescence lifetime imaging microscopy (FLIM), single-molecule localization microscopy (SMLM) and 2-photon microscopy, among others, are compatible with high-speed super-resolution imaging, and have been used in studies of TCR and B cell receptor (BCR) microcluster dynamics, recruitment and phosphorylation of signaling kinases, and IS proximal cytoskeleton dynamics [93–97]. Moreover, some studies of single-molecule dynamics have further been coupled with FRET biosensors and fluorescent gene reporters, such as TCR α -GFP [98] and NFAT-FP [99], to image dynamic processes during T cell activation. For example, a FRET biosensor was developed to image TCR-pMHC interactions, deriving the dissociation and association rates of TCR-pMHC complexes on a modified planar lipid bilayer system [100]. Clif, a FRET biosensor that can specifically bind with CD3 ζ in TCR-CD3 clusters, was also developed to measure monomers and protein clusters in Jurkat T cells; the results showed that CD3 ζ -Clif molecules formed larger and more compacted clusters upon T cell activation [101]. In another study, a FRET pair for detecting the interactions between ZAP-70 and phosphorylated CD3 enabled visualization of activation-dependent CD3 ζ in Jurkat T cells [102]. Apart from imaging these protein interactions, the activity of the protein kinases, Lck and Fyn, has also been monitored via a FRET system comprising an enzyme-sensitive substrate peptide as sensing moiety, and the Src homology 2 (SH2) motif domains interacting with the phosphorylated substrate peptide to alter FRET efficiency [103,104]. These examples of imaging techniques indicate the unique capacity of directly observing activation timelines in T cells, which can also help us to better understand T cell functions in basic and translational immunology.

intracellular ATP concentrations via ATP assays and the evaluation of bioenergetic metabolism via **Seahorse assays** [18], insufficiently inform on the possibility of cancer prognoses or putative treatments. Here, we describe some of the metabolic targets that can be assessed via molecular imaging.

Pyruvate

The conversion of isotopically labeled glucose to pyruvate and lactate allows the measurement of intracellular glycolytic flux. This can be detected through two different methods: **β -counting** for ^{14}C -pyruvate and ^{14}C -lactate generated via ^{14}C -glucose [19], and ^{13}C nuclear magnetic resonance spectroscopy/imaging for metabolic products of ^{13}C -glucose [20]. The latter has been used for *in vivo* applications, such as ^{13}C -pyruvate magnetic resonance spectroscopy to evaluate the influence of agmatine on brain metabolism in a type 2 diabetes mellitus mouse model [21], although its limited sensitivity hampers its practical use [22]. Nevertheless, **hyperpolarized ^{13}C MRI** can improve the ^{13}C signal intensity to meet the requirement for clinical applications and be used for detecting metabolic responses to chemohormonal therapy in cancer [23,24]. This method has been used for not only detecting the flux from pyruvate to lactate in human CD4 $^{+}$ T cells *in vitro* [25], but also monitoring the conversion of ^{13}C -pyruvate to ^{13}C -lactate in patients with prostate cancer in a Phase 1/2 clinical trial (NCT02913131)ⁱ (Table 2) [26]. Unlike **2-deoxy-2-(^{18}F)fluoro-D-glucose (^{18}F -FDG) PET imaging**, which differentiates the glucose uptake of cancerous versus normal tissues, hyperpolarized ^{13}C MRI, apart from its nonradioactive nature, can differentiate glycolytic metabolism from oxidative phosphorylation [23,24].

dCK/dGK

Highly expressed in acute leukemia cells and activated lymphocytes, nucleotide salvage pathway rate-limiting enzymes, such as deoxycytidine kinase (dCK) and deoxyguanosine kinase (dGK), can be considered as putative targets for cancer therapy and imaging [27]. The first PET imaging probe targeting dCK, 1-(2'-deoxy-2'-[^{18}F]fluoro- β -D-arabinofuranosyl) cytosine ([^{18}F]-FAC), was used to study the proliferation of CD8 $^{+}$ T cells in spleen and tumor-draining lymph nodes

within the tumor may harbor different mutations or characteristics. This heterogeneity can affect the tumor response to treatment.

Linker for activation of T cells (LAT): transmembrane adaptor protein with a crucial role in T cell activation. LAT is phosphorylated upon TCR engagement, recruiting downstream signaling molecules, such as PLC γ -1 and ADAP, to initiate T cell activation.

Seahorse assay: used to measure the metabolic activity of cells, measuring the rate of oxygen consumption and extracellular acidification, indicators of mitochondrial respiration and glycolysis, respectively.

Semiconducting polymer nanoreporters: class of nanomaterials comprising semiconducting polymer nanoparticles or nanowires that exhibit unique optical and electronic properties, making them useful as sensors and reporters to detect biomolecules, monitor cellular processes, and track drug delivery.

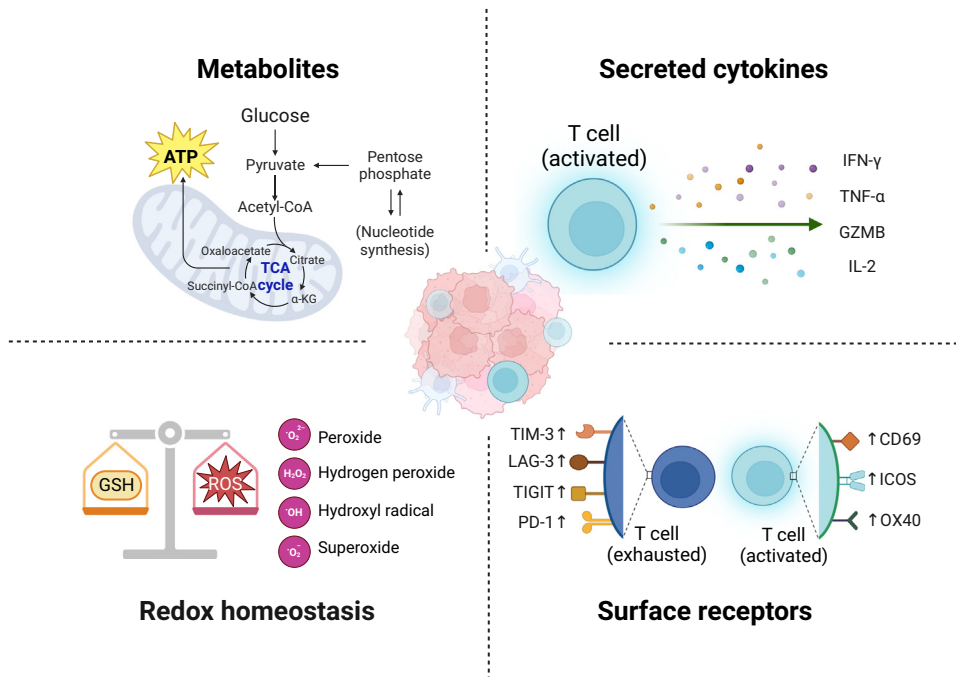
Single-chain variable fragment (ScFv): fusion protein of the variable regions of the heavy (V_H) and light chains (V_L) of immunoglobulins, connected with a short linker peptide of 10–25 amino acids; it retains the specificity of the original immunoglobulin, despite removal of the constant regions and the introduction of the linker.

T1 relaxation time: used to determined how quickly the nuclei in a sample return to their equilibrium or aligned state after being perturbed by an external magnetic field in MRI. It is different for various types of tissue and substance, providing important information for MRI analyses.

T cell immune synapse (IS): highly specialized structure formed between T cells and APCs during an immune response; contains a central cluster of receptors and signaling molecules, allowing efficient communication between the cells.

Key figure

Examples of targets used for *in vivo* visualization of T cell phenotypes and activities.



Trends in Immunology

Figure 3. Non-invasive molecular imaging strategies were utilized to monitor T cell activity *in vivo*, providing certain timely predictions of tumor response to immunotherapy. Advanced molecular imaging probes can be designed to target various biomarkers associated with T cell activation or exhaustion, including T cell metabolism, redox status, surface receptor expression, and secreted molecules, among others. Abbreviations: GZMB, granzyme B; ICOS, inducible T cell co-stimulator; IFN, interferon; IL, interleukin; LAG-3, lymphocyte-activation gene 3; PD-1, programmed cell death-1; TCA, tricarboxylic acid; TIGIT, T cell immunoreceptor with Ig and ITIM domains; TIM-3, T cell immunoglobulin and mucin domain-3; TNF- α , tumor necrosis factor- α . Figure created using BioRender ([biorender.com](https://www.biorender.com)).

(TDLNs) in a Moloney murine sarcoma virus (MoMSV)-induced mouse sarcoma model that was established on B6.MRL-*Fas^{lpr}*/J mice [28]. It has also been tested in a Phase 1 clinical trial assessing the biodistribution of [^{18}F]-FAC in healthy subjects and patients with cancer or autoimmune/inflammatory diseases (NCT01180907)ⁱⁱ. Subsequently, other PET probes for targeting dCK and dGK, such as L- [^{18}F]-FAC and 1-(2'-deoxy-2'- [^{18}F]fluoro-5-methyl- β -L-arabinofuranosyl) cytosine (L- [^{18}F]-FMAC), have emerged [29,30]. However, these FAC-based probes are rapidly catabolized by cytidine deaminase and cross-react with mitochondrial thymidine kinase 2 (TK2) *in vivo*, as evidenced by the phosphorylation of deoxythymidine by mitochondrial-TK purified from HeLa cells (cytosolic *TK^{-/-}* relative to wild-type) [31].

By contrast, probes based on purine analogs, such as 2-chloro-2'-deoxy-2'- [^{18}F]fluoro-9- β -D-arabinofuranosyl-adenine ([^{18}F]-CFA) and 2'-deoxy-2'- [^{18}F]fluoro-9- β -D-arabinofuranosyl-guanine ([^{18}F]-AraG), are not phosphorylated by TK2 in NSG mice bearing CCRF-CEM tumors [32,33]. In another study, [^{18}F]-CFA PET was combined with contrast-enhancement MRI to differentiate tumor progression from pseudoprogression in glioblastoma (GBM)-tumor bearing mice receiving dendritic cell (DC) vaccination and/or PD-1 monoclonal antibodies (mAbs) ICB [34]. [^{18}F]-AraG was

Table 1. Molecular imaging for visualizing T cell activity *in vivo*^a

Target	Biomarker	Imaging	Probe	Experimental model	Refs	
Metabolism	Pyruvate	MRI	HP ¹³ C-pyruvate	Prostate cancer in humans	[26]	
	dCK	PET	[¹⁸ F]-FAC	MoMSV-induced sarcoma in B6.MRL-Fas ^{lpr} /J mice	[28]	
			L-[¹⁸ F]-FAC	L1210 tumors in mice	[29]	
			L-[¹⁸ F]-FMAC			
			[¹⁸ F]-CFA	CCRF-CEM tumors in NSG mice	[32]	
				GL261 tumors in mice	[34]	
	dCK, dGK	PET		[¹⁸ F]F-AraG	M38 tumors in mice	[35]
				MC38, A9F1, among other tumors in mice	[36]	
Redox status	-SS-	MRI	T-Fulips	4T1 tumors in mice	[43]	
	O ₂ ⁻	FL	SPNRs	4T1 tumors in mice	[45]	
Surface receptors	PD-1	PET/FL	⁶⁴ Cu-DOTA-PD-1	B16F10 tumors in <i>Foxp3</i> +LuciDTR4 mice	[48]	
			PET	PD-1- ⁶⁴ Cu/IRDye800CW	4T1 tumors in mice	[49]
		PET	⁸⁹ Zr- nivolumab	A549 tumors in NSG mice	[50]	
			⁸⁹ Zr-pembrolizumab	NSCLC in humans	[52]	
	OX40	FL	IRDye800-AbOX40	H22 tumors in mice	[54]	
		PET	⁶⁴ Cu-DOTA-AbOX40	A20 tumors in mice	[55]	
				Graft-versus-host disease in mice	[56]	
	ICOS	PET	⁸⁹ Zr-DFO-ICOS	A20 tumors in mice	[58]	
				LLC tumors in mice	[59]	
	CD69	SPECT	¹¹¹ In-DOTA-ZCD _{69.4}	Healthy rats	[60]	
		PET	⁸⁹ Zr-DFO-CD69	CT26 tumors in mice	[61]	
				GL261 tumors in mice	[62]	
	TIGIT	PET	⁶⁸ Ga-GP12	B16F10 tumors in mice and NSCLC in humans	[63]	
	TIM-3	PET	⁶⁴ Cu-NOTA-RMT3-23	NSCLC in humans	[64]	
	LAG-3	PET	⁸⁹ Zr-DFO-REGN3767	MC38 tumors in mice	[66]	
⁸⁹ Zr-BI754111			NSCLC and head and neck squamous cell carcinoma in humans	[67]		
Secreted molecules	GZMB	PET	⁶⁸ Ga-NOTA-GZP	CT26 tumors in mice	[68]	
		FL	GNR	MC38 and B16F10 tumors in mice	[69]	
			GrB nanosensors	Skin isografts and allografts in mice	[70]	
			TMAP _{CTL}	4T1 and CT26 tumors in mice	[71]	
			⁶⁴ Cu-GRIP B	CT26, MC38, and EMT6 tumors in mice	[72]	
	IFN-γ	PET	⁸⁹ Zr-anti-IFN-γ	TUBO tumors in mice	[74]	
				CT26 tumors in mice	[75]	
	IL-2	PET		[¹⁸ F]FB-IL2	hPBMCs inoculated in CB17.Cg- <i>Prkdc</i> ^{scid} <i>Lys</i> ^{tg-J} /Crl mice	[78]
					TC-1 tumors in mice	[79]
					Metastatic melanoma in humans	[80]
SPECT		^{99m} Tc-HYNIC-IL2	Stage IV malignant melanoma in humans	[81]		
PET		⁶⁸ Ga-NODAGA-IL2	hPBMCs inoculated in CB17.Cg- <i>Prkdc</i> ^{scid} <i>Lys</i> ^{tg-J} /Crl mice	[82]		
			¹⁸ F-AIF-RESA-IL2			

^aAbbreviations: dCK, deoxycytidine kinase dGK, deoxyguanosine kinase; GZMB, granzyme B; ICOS, inducible T cell co-stimulator; IFN, interferon; IL, interleukin; LAG-3, lymphocyte-activation gene 3; PD-1, programmed cell death-1; TIGIT, T cell immunoreceptor with Ig and ITIM domains; TIM-3, T cell immunoglobulin and mucin domain-3.

Table 2. Imaging probes in clinical trials for PET and MRI^a

Probe	Trial design	Subject	No. of patients	Clinicaltrials.gov ID
HP ¹³ C-pyruvate MRI	Interventional Phase 1/2 Nonrandomized	Prostate cancer	23	NCT02913131 ⁱ
[¹⁸ F]-FAC PET	Observational Nonprobability	Cancer Inflammation Healthy	10	NCT01180907 ⁱⁱ
[¹⁸ F]F-AraG PET	Interventional Open-label	NSCLC	10	NCT05157695 ^{iv}
[¹⁸ F]F-AraG PET	Interventional Phase 2 Open-label	Non-Hodgkin lymphoma	6	NCT05096234 ^v
⁸⁹ Zr-pembrolizumab PET	Interventional Open-label	Melanoma NSCLC	18	NCT02760225 ^v
⁸⁹ Zr-DFO-REGN3767 PET	Interventional Early Phase 1 Randomized	Large B cell lymphoma Diffuse large B cell lymphoma	20	NCT04566978 ^{vi}
⁸⁹ Zr-DFO-REGN3767 PET	Interventional Phase 1/2 Nonrandomized	Metastatic solid tumor	38	NCT04706715 ^{vi}
[⁸⁹ Zr]Zr-BI 754111 PET	Interventional Phase 1 Nonrandomized	Carcinoma NSCLC Head/neck neoplasms	8	NCT03780725 ^{viii}
[¹⁸ F]FB-IL-2 PET	Interventional Open-label	Melanoma	19	NCT02922283 ^{ix}
^{99m} Tc-HYNIC-IL-2 SPECT	Interventional Early Phase 1 Nonrandomized	Stage IV skin melanoma	5	NCT01789827 ^x

^aAbbreviation: NSCLC, nonsmall cell lung cancer.

also reported to be phosphorylated by cytoplasmic dGK and dCK, which then accumulated in activated CD8⁺ and CD4⁺ T cells, allowing the prediction of the therapeutic efficacy of anti-PD-1 mAb ICB through differential [¹⁸F]F-AraG signals in tumors and TDLNs from rhabdosarcoma-bearing mouse responders versus nonresponders [35]. Moreover, [¹⁸F]F-AraG has been used to determine the number of tumor-infiltrating PD-1⁺CD8⁺ T cells *in vivo* in response to combined chemotherapy (e.g., oxaliplatin/cyclophosphamide and paclitaxel/carboplatin in a panel of tumor-bearing mouse models). Specifically, the authors reported a significant correlation between the signal and number of PD-1⁺CD8⁺ T cells isolated from the tumors; moreover, oxaliplatin/cyclophosphamide treatment led to close to a 2.4-fold higher signal compared with controls [36]. Currently, [¹⁸F]F-AraG PET imaging is being tested in clinical trials; for example, a Phase 1 clinical trial (NCT05157695)ⁱⁱⁱ to visualize tumor infiltrating T cell activation in nonsmall cell lung cancer (NSCLC), and a Phase 2 clinical trial (NCT05096234)^{iv} evaluating the immunological response to CAR-T therapy in lymphoma. Both trials are recruiting patients.

Redox-related targets

The TME is characterized by an elevated amount of ROS [37]. Combining immunotherapy with radiotherapy can increase the concentration of ROS to enhance tumor cell elimination [38]. However, excessive ROS may induce redox-induced homeostatic imbalance in T cells, which can also negatively affect the lifespan and effectiveness of activated T cells [39]. Thus, targeting ROS might represent a putative strategy for imaging and evaluating T cell activity.

Reciprocal transformation of thiol and disulfide

The presence of thiol (-SH) groups on the T cell membrane depends on reduced thioredoxin (Trx) [40] and surface CD4 molecules [41]. When the TME becomes more oxidative and abundant in ROS, -SH groups can be converted to disulfide (-SS-) bonds, inhibiting the membrane surface-specific antigenic activity and T cell functions [42]. By targeting surface -SH in T cells, a novel probe, T-Fulips, was developed for imaging and modulating T cell activity [43]. T-Fulips contains F(ab')₂ fragments of anti-CD3 mAbs to specifically target T cells, as well as the ROS scavenger 2,2,6,6-tetramethyl-4-piperidinone (TEMP), preventing -SH groups from being converted into -SS- bonds on T cells. The oxidation of TEMP to 2,2,6,6-tetramethylpiperidiny-1-oxide (TEMPO) provides an antimagnetic to paramagnetic change, which is detectable by MRI. Thus, the magnetization state of T-Fulips can reflect the quantity of surface -SH groups and, indirectly, aspects of T cell activation *in vivo*. Specifically, in 4T1 tumor-bearing mice, intravenous delivery of T-Fulips resulted in significantly higher tumor-infiltrating CD4⁺ and CD8⁺ T cell activity in mice receiving 4 Gy X-ray irradiation compared with controls, as indicated by changes in **T1 relaxation time** in tumors compared with those of the isotype-Fulips control group. Moreover, in this study, T-Fulips was applied to enhance the therapeutic efficacy of OT-1 mouse CD8⁺ adoptive T cell transfer against melanoma B16F10-OVA tumors; this suggested that T-Fulips can be used as strategy to image and assess T cell activity in cancer theranostics [43].

Intracellular O₂⁻

As the main ROS, the superoxide anion (O₂⁻) can activate T cells [44]. For O₂⁻ detection, **semi-conducting polymer nanoreporters (SPNRs)** displaying O₂⁻-activatable chemiluminescence were developed for *in vivo* imaging of immune activation during cancer immunotherapy [45]. The SPNRs comprised a semiconductor polymer and a caged chemiluminescent phenoxy-doxetane substrate, representing the chemiluminescent receptor and donor, respectively. Stronger chemiluminescent signals were observed from cytotoxic CD8⁺ T cells compared with those from 4T1 cells and normal cells *in vitro* due to the higher concentration of intracellular O₂⁻ in T cells, which is required for T cell activation [46]. Moreover, after SPNR injection, an enhanced fluorescence signal was detected in tumors of 4T1 tumor-bearing mice treated with either S-(2-boronoethyl)-L-cysteine hydrochloride (BEC) or PBS. However, only tumor tissues from mice pretreated with BEC exhibited an enhanced chemiluminescence signal due to the elevated O₂⁻ concentrations in helper CD4⁺ T cells and cytotoxic T lymphocytes (CTLs), compared with those from the PBS control group. Although the limited penetration depth of optical signals may hamper the practical application of the above reporting system, it remains useful for screening immunotherapeutic drugs in preclinical studies.

Surface receptors as targets

T cells express a range of surface receptors that interact with ligands to trigger intracellular signaling pathways. Some highly and stably expressed surface receptors are suitable for monitoring T cell activity as imaging targets, particularly receptors involved in tumor immunity and immune response modulation.

PD-1

PD-1 is a well-known immune checkpoint receptor that is present on the surface of T cells and is upregulated during chronic infections and cancer. When PD-L1 on tumor cells binds PD-1, it suppresses T cell activation, allowing the tumor to evade the immune system. Thus, PD-1 and PD-L1 blockers can reactivate the immune function of TILs by blocking the PD-L1/PD-1 signaling pathway in certain tumors [47]. Thus, the expression of PD-1 becomes a potential indicator of the immune reactivation of CD8⁺ T cells. PD-1 blockers make a significant contribution to ICB therapy and there is growing interest in molecular imaging probes targeting PD-1 for monitoring T cell

activity. For instance, a ^{64}Cu -DOTA-PD-1 PET tracer was fabricated for imaging PD-1 expression on TILs and lymphoid organs in *Foxp3*⁺LuciDTR4 mice bearing B16F10 melanoma tumors [48]. Moreover, a PET/FL dual-modality probe targeting PD-1, namely the PD-1-liposome-DOX- ^{64}Cu /IRDye800CW, was used for imaging and evaluating the activity of tumor-infiltrating CD8⁺ T cells in 4T1 tumor-bearing mice [49]. In addition, PD-1 **immunoPET** imaging was carried out using a ^{89}Zr -labeled PD-1 tracer. Specifically, ^{89}Zr -nivolumab was applied to track PD-1-expressing T cell infiltration in tumors of A549-bearing NSG mice [50] and in patients with advanced NSCLC [51]. These studies showed that tumor uptake of the PET probe correlated with the number of PD-1⁺ TILs, enabling non-invasive evaluation of PD-1 expression in mice and patients with NSCLC [50,51]. Moreover, a positive correlation was observed between the accumulation of ^{89}Zr -pembrolizumab in tumors and the response of anti-PD-1 mAb therapy in patients with metastatic melanoma and NSCLC (NCT02760225)^y [52]. Patients with higher uptake of ^{89}Zr -pembrolizumab in tumors showed improved survival rates compared with those showing low probe uptake. Overall, the PD-1 tracer remains the primary choice for PET imaging, despite the caveat that PD-1 is not solely expressed by T cells.

OX40

OX40 is a receptor that belongs to the tumor necrosis factor receptor superfamily and is mainly present in activated T cells. When OX40 binds the OX40 ligand, it stimulates activation of CD8⁺ T cells during immune responses against tumors, suggesting that OX40 expression is strongly associated with T cell activation [53]. To predict the response to immunotherapy in tumors using OX40 imaging, a near-infrared FL imaging probe IRDye800-AbOX40 was developed; it imaged activated CD3⁺ T cells in the tumors of H22 tumor-bearing mice after receiving CpG intratumoral vaccination [54]. In a similar way, an OX40-specific PET tracer (i.e., ^{64}Cu -DOTA-AbOX40) was reported to predict tumor responses to *in situ* CpG vaccination in A20 tumor-bearing mice [55]. Relative to vehicle-treated controls, significantly enhanced PET signals were observed in the tumors and spleen 2 days and 9 days post treatment, reflecting an early and late tumor response to CpG, respectively. Moreover, this study reported that OX40 PET imaging provided higher accuracy of T cell activation compared with commonly used invasive tests, such as the measurement of cytokines in the blood [55]. Additionally, OX40-targeted PET imaging was used for early diagnosis of acute graft-versus-host disease (GVHD) in a histocompatibility complex (MHC)-mismatch murine model, before the manifestation of noticeable clinical symptoms; this study also reported excellent sensitivity and specificity in detecting OX40 expression in spleen and mesenteric lymph nodes (MLNs) [56].

ICOS

The expression of inducible T cell co-stimulator (ICOS) is specifically induced in activated T cells [57]. ICOS immunoPET imaging was utilized to detect ICOS expression, assessing T cell activity. A suitable probe, ^{89}Zr -DFO-ICOS, comprising ^{89}Zr and an ICOS mAb was shown to elicit stronger signals compared with controls in the bone marrow of A20 tumor-bearing mice receiving CAR-T cell therapy, indicating that ICOS-immunoPET imaging could be used for monitoring CAR-T cell activation *in vivo* [58]. In addition, ^{89}Zr -DFO-ICOS mAb-based PET imaging was performed on Lewis lung cancer (LLC) tumor-bearing mice treated with different immunotherapies, such as PD-1 ICB, or a stimulator of interferon genes (STING) agonist; ICOS-immunoPET imaging could predict an early therapeutic response. Greater CD4⁺ and CD8⁺ T cell activation in the tumors was detected by ^{89}Zr -DFO-ICOS PET imaging after STING agonist treatment, which was consistent with the stronger inhibition of tumor growth relative to PBS or PD-1 ICB alone. Altogether, these results suggest that ICOS tracking can help assess T cell behaviors and, ideally, could help predict the efficacy of immunotherapies [59], although this warrants further and robust investigation.

CD69

CD69 is an early-activation marker highly expressed on CTLs and natural killer (NK) cells. Targeting CD69 has been proposed as an alternative way for visualizing T cells *in vivo*. For example, a cross-reactive CD69-binding Z variant $Z_{CD69:4}$, generated by *Escherichia coli*, was chosen to image T cells in rats through ^{111}In , chelated by 1,4,7,10-tetraazacyclododecane-N,N',N'',N'''-tetraacetic acid (DOTA) [60]. ^{111}In -DOTA- $Z_{CD69:4}$ exhibited optimal chemical stability, high affinity, and specificity for human and murine CD69, making it a promising probe for imaging activated T cells. Moreover, a CD69 immunoPET imaging probe ^{89}Zr -DFO-H1.2F3, comprising a highly specific CD69 mAb H1.2F3 and radiolabeled with ^{89}Zr , was developed to differentiate responders from nonresponders to combined immunotherapy with anti-PD-1 and anti-CTLA-4 mAbs in CT26 tumor-bearing mice [61]. In another study, a ^{89}Zr -DFO-CD69 mAb PET tracer was adopted to assess the responses to combined immunotherapy using anti-CTLA-4 and anti-PD-1 mAbs in GL261-bearing mice. The results showed a significantly higher uptake of the tracer in the tumors of ICB-treated mice than in controls [62]. The above studies suggest that CD69 immunoPET imaging offers sufficient sensitivity for monitoring T cell accumulation and/or activity *in vivo* in predicting tumor responses to immunotherapy, although extensive studies are required before further clinical applications can be considered.

Other receptors

PET imaging of other inhibitory receptors on T cells, such as lymphocyte-activation gene 3 (LAG-3), T cell immunoreceptor with Ig and ITIM domains (TIGIT), and T cell immunoglobulin and mucin domain-3 (TIM-3), has also been investigated for *in vivo* visualization of T cell activity. A ^{68}Ga -labeled peptide (^{68}Ga -GP12) ligand of TIGIT was designed for TIGIT immunoPET imaging in B16F10 melanoma tumor-bearing mice; the results showed that tumor uptake of ^{68}Ga -GP12 positively correlated with TIGIT expression on CD4^+ and CD8^+ T cells in tumors [63]. This suggested that ^{68}Ga -GP12 can be used for imaging T cell changes *in vivo* and for predicting the therapeutic efficacy of anti-TIGIT mAb therapy via PET [63]. Moreover, a ^{64}Cu -NOTA-RMT3-23 ligand of TIM-3 coupled to a specific anti-TIM-3 mAb was developed to delineate TIM-3 expression in B16F10 tumor-bearing mice before and after radiotherapy [64]. With the aid of this probe, the distribution of $\text{TIM-3}^+\text{CD45}^+$ lymphocytes in the peritumoral regions of a mouse melanoma were visualized, suggesting the feasibility of ^{64}Cu -NOTA-RMT3-23 immunoPET in tracking TIM-3, which might help optimize clinical TIM-3-targeted immunotherapies. In terms of LAG-3, 15 antibodies have been developed for LAG-3 ICB [65], as well as some LAG-3 PET tracers. An early Phase 1 clinical trial (NCT04566978)^{vi} and a Phase 1/2 clinical trial (NCT04706715)^{vii} of ^{89}Zr -DFO-REGN3767 (anti LAG-3) PET imaging are recruiting patients with relapsed/refractory diffuse large B cell lymphoma (DLBCL) and certain advanced solid tumors, respectively [66]. In addition, ^{89}Zr -BI754111 (NCT03780725)^{viii} has been clinically investigated in a Phase 1 clinical trial (NCT03780725)^{viii} in patients with advanced NSCLC or head and neck cancer, pretreated with BI 754091 [67]. The results demonstrated that tumor uptake of the tracer correlated with TIL infiltration, suggesting that LAG-3 harbors potential as a target when following TIL responses during this type of candidate immunotherapy.

Cytokines as targets

When T cells recognize tumor antigen presented by antigen-presenting cells (APCs), they undergo activation, releasing a range of effector cytokines and cytotoxic molecules, helping to induce tumor cell death as well as regulating the activation, proliferation, and effector function of different immune cell types.

Granzyme B

Granzyme B (GZMB) is a type of serine protease secreted by cytotoxic T cells and NK cells during cellular immune activation. To monitor cytotoxic T cell activity *in vivo*, a GZMB-specific PET

imaging agent (^{68}Ga -NOTA-GZP) was developed [68]. When intravenously injected into mice bearing CT26 tumors, the ^{68}Ga -NOTA-GZP radiotracer was demonstrated to specifically and quantitatively target GZMB in tumors that were treated with anti-PD-1/anti-CTLA-4 mAb combined therapy; this allowed monitoring of T cell activation in response to immunotherapy [69]. Moreover, a GZMB nanoreporter (GNR) comprising a polymeric backbone (polyisobutylene-alt-maleic anhydride, PIMA), an immunotherapeutic mAb (anti-PD-L1), and a GZMB-responsive imaging probe, was designed for monitoring the early tumor response to immunotherapy [69]. The signal of GZMB-responsive FL imaging in mouse tumors treated with PDL1-GNR was higher than that of IgG-GNR controls, due to anti-PD-L1-mediated immune activation. Moreover, this probe could discriminate between highly (MC38) and poorly immunogenic (B16F10) tumor-bearing mice via real-time monitoring of T cell activity *in vivo*. In another study, a GZMB-responsive FL imaging nanosensor was developed for the early detection of the onset of transplant rejection in skin-graft rejection mouse models; the nanosensor was found largely accumulated in allograft tissues rather than in isograft tissues [70]. Others reported tandem-activatable molecular probes (TAMP_{CTL}) capable of dynamically monitoring the activity of tumor-infiltrating CTLs in 4T1 and CT26 tumor-bearing mice in response to combined anti-PD-L1 and anti-CD47 mAb immunotherapy [71]. Apart from GZMB-based FL imaging, T cell activation was also monitored via ^{64}Cu -GRIP B-mediated PET imaging. Higher tumor uptake of the ^{64}Cu -GRIP B probe was observed in a panel of mouse tumor models and correlated with tumor volume changes upon anti-CTLA-4 and anti-PD-1 mAb combination ICB [72]. These results suggest that GZMB enzyme-based *in vivo* imaging can be used for predicting certain early tumor responses to immunotherapy, although further work is necessary.

Interferon- γ

Interferon (IFN)- γ is a key effector cytokine secreted by activated T cells, which can potentiate the antitumor immune response through diverse mechanisms [73]. A ^{89}Zr radiolabeled anti-IFN- γ mAb was first developed for PET imaging of IFN- γ in TUBO tumor-bearing mice receiving human epidermal growth factor receptor 2 (HER2)/neu DNA vaccine, evaluating immune responses by monitoring the uptake of the IFN- γ PET probe in the tumors [74]. Compared with total CD3⁺ TIL imaging, the T cell activation status was better assessed via IFN- γ immunoPET, exhibiting reduced off-target binding to secondary lymphoid tissues, thus providing valuable non-invasive insights into T cell effector functions *in vivo*. Higher uptake of radiotracer was observed in vaccinated tumors than in controls, which was inversely correlated with tumor growth rate; this suggested that IFN- γ PET imaging can be considered a potential predictive tool for monitoring responses to immunotherapy. Additionally, a lead diabody (Db) targeting IFN- γ was developed using ^{89}Zr labeling and two distinct **single-chain variable fragments (scFvs)** V_H and V_L. This diabody was designed with an optimal length of peptide linker for PET imaging of IFN- γ in CT26 tumor mice, overcoming the limitations of using full-length anti-IFN- γ mAbs [75].

Interleukin-2

Interleukin (IL)-2 secreted by many immune cells influences the development and differentiation, proliferation, and effector function of T cells by binding to the IL-2 receptor on T cells [76]; it has pro- or anti-inflammatory effects depending on the subset of targeted cells [77]. In one study, [^{18}F]FB-IL2 was generated by labeling IL-2 with N-succinimidyl-4- ^{18}F -fluorobenzoate; the tracer showed no significant difference from native IL-2 in stimulation assays *in vitro*; it was also used to detect the migration of human peripheral blood mononuclear cells (hPBMCs) in SCID beige (CB17.Cg-Prkdc^{scid}Lyst^{tg-J}/Cr) mice through PET imaging *in vivo* [78]. In another study, [^{18}F]FB-IL2 PET imaging was performed to non-invasively monitor tumor infiltration of activated CD8⁺ T cells in TC-1 tumor-bearing mice receiving 14 Gy radiotherapy alone or in combination with SFVeE6,7 immunization [79]. A significantly higher [^{18}F]FB-IL-2 uptake in tumors following

treatment was observed via PET imaging relative to untreated mice [79]. However, PET imaging of patients with stage IV metastatic melanoma in a nonrandomized clinical trial did not show a correlation between [^{18}F]FB-IL2 uptake in tumor lesions and subsequent responses during combined anti-PD-1 and anti-CTLA-4 ICB, or monotherapy (NCT02922283)^{ix}, suggesting that these results can be variable [80]. Of note, a $^{99\text{m}}\text{Tc}$ -HYNIC-IL2 SPECT imaging probe was used to detect CD3⁺ TILs in tumors, as well as the size of metastatic lesions, in patients with metastatic melanoma following combined anti-PD-1 and anti-CTLA-4 ICB in a completed early Phase 1 clinical trial (NCT01789827)^x. TIL tumor infiltration and tumor dimension positively correlated with tumor uptake of $^{99\text{m}}\text{Tc}$ -HYNIC-IL2, suggesting pseudoprogression due to increased TIL infiltration after treatment [81]. Another study reported the use of IL-2 radiolabeled tracers, such as ^{18}F -AIF-RESA-IL-2 and ^{68}Ga -NODAGA-IL-2, for PET imaging of activated hPBMCs following inoculation into SCID beige (CB17.Cg-Prkdc^{scid}Lyst^{bg-J}/Cr1) mice [82]. The results indicated high uptake of ^{18}F -AIF-RESA-IL-2 in hPBMC xenografts and lymphoid tissues, suggesting the potential for this tracer for detecting activated immune cells *in vivo*.

Concluding remarks

The field of molecular imaging and monitoring of T cell activity *in vivo* is progressing; it encompasses examining targets that are closely associated with T cell metabolism, redox status, surface receptor expression, and secreted molecules, among others. In addition, real-time imaging of T cells, sometimes accompanied by assessing the regulation of T cell functions upon elegant probe designs, can be helpful for evaluating early tumor responses, stages, and treatment stratifications, moving toward approaches of personalized medicine. In this context, an accurate and comprehensive assessment of T cell activity during immunotherapy will become pivotal. Nevertheless, the underlying biological mechanisms leading to changes in T cell activity are complex and evidently require further in-depth research. Specific biomarkers that are associated with T cell activation status must also be rigorously investigated. Of note, the vastly unknown heterogeneity of immune responses in patients with cancer, in addition to the heterogeneity of different lesions within the same patient, make it even more difficult to non-invasively monitor therapeutic efficacy (see [Outstanding questions](#)).

Concerning different imaging modalities, clinical imaging methods, including PET and MRI, have and are currently being used in several clinical trials. However, although FL imaging has yet to be used in clinical trials to our knowledge, other optical imaging strategies are offering powerful tools for fundamentally understanding immune responses; these include total internal reflection fluorescence microscopy (TIRFM), **fluorescence resonance energy transfer (FRET)**, 2-photon intravital microscopy in animal models, as well as super-resolution, single-molecule imaging methods [83–85]. The sensitivity and specificity of various molecular imaging probes remain hot topics of debate, including their safety in clinical applications. We argue that combining imaging with assessing the regulation of T cell activity is an attractive approach for clinical advancements in immuno-oncology, and one that awaits further exploration. Nevertheless, pharmacokinetic behaviors and regulating moieties for imaging must be matched. Overall, because imaging T cell activity *in vivo* during immunotherapy is a rapidly growing field, we anticipate that it may hold great promise for advancing tumor treatments.

Acknowledgments

We acknowledge the financial support from the National Natural Science Foundation of China (82130059, 81720108024, 22122407, 12075164), Tang Scholar Program, the Open Project Program of the State Key Laboratory of Radiation Medicine and Protection (GZK12023025), and the Science and Technology Project from Suzhou City (KJXW2022024, SYS2020169) and a project funded by the Priority Academic Program Development of Jiangsu Higher Education Institutions.

Outstanding questions

How do we evaluate the efficacy of immunotherapy in a timely and precise manner? Detection of T cell infiltration, tumor mutational burden (TMB), and PD-L1 expression has been used to differentiate certain responders from nonresponders in the clinic. However, various inconsistencies occur with unclear mechanisms.

What are the underlying mechanisms inducing T cell dysfunction? Constant antigenic stimulation, nutritional restriction, oxidative stress, and other immunosuppressive factors can influence T cell activity, and may contribute to T cell exhaustion. How these integrate into a regulatory framework remains to be further investigated.

Can reversing T cell exhaustion improve tumor responses to immunotherapy in more cancers? The transformation of T cells from activation to exhaustion is dynamic, involving multiple interconnected subpopulations, such as progenitor and terminally exhausted T cells. The subset(s) of activated and exhausted T cells that are most relevant during immunotherapy await further in-depth analysis.

How do we build more sensitive and specific imaging probes to monitor T cell activation? The moderate affinity of antibodies that are largely used as targeting molecules, the limited penetration depth of FRET-based probes, and the unsatisfactory retention time of small molecule-based probes limit current imaging probes assessing T cell activity.

How do we improve the specificity of imaging probes for T cell activity? The biomarkers chosen for constructing imaging probes are not specific enough for T cells and some of them are related to NK cells, such as certain surface receptors, metabolites, and secreted cytokines. Thus, other specific biomarkers for T cell activation and exhaustion remain to be further explored.

Can the dynamic interactions between T cells and target cells be visualized during immune treatments *in vivo*? Organoids mimicking the tumor immune microenvironment may offer a useful tool to further study T cell interactions in intact tissues through 3D imaging.

Declaration of interests

None declared by authors.

Resources

ⁱ<https://clinicaltrials.gov/ct2/show/NCT02913131>

ⁱⁱ<https://clinicaltrials.gov/ct2/show/NCT01180907>

ⁱⁱⁱ<https://clinicaltrials.gov/ct2/show/NCT05157659>

^{iv}<https://clinicaltrials.gov/ct2/show/NCT05096234>

^v<https://clinicaltrials.gov/ct2/show/NCT02760225>

^{vi}<https://clinicaltrials.gov/ct2/show/NCT04566978>

^{vii}<https://clinicaltrials.gov/ct2/show/NCT04706715>

^{viii}<https://clinicaltrials.gov/ct2/show/NCT03780725>

^{ix}<https://clinicaltrials.gov/ct2/show/NCT02922283>

^x<https://clinicaltrials.gov/ct2/show/NCT01789827>

References

- Wang, Y. *et al.* (2022) Immune checkpoint modulators in cancer immunotherapy: recent advances and emerging concepts. *J. Hematol. Oncol.* 15, 111
- Adachi, K. *et al.* (2018) IL-7 and CCL19 expression in CAR-T cells improves immune cell infiltration and CAR-T cell survival in the tumor. *Nat. Biotechnol.* 36, 346–351
- Hegde, P.S. and Chen, D.S. (2020) Top 10 challenges in cancer immunotherapy. *Immunity* 52, 17–35
- Philip, M. and Schietinger, A. (2022) CD8⁺ T cell differentiation and dysfunction in cancer. *Nat. Rev. Immunol.* 22, 209–223
- Vignali, P.D.A. *et al.* (2023) Hypoxia drives CD39-dependent suppressor function in exhausted T cells to limit antitumor immunity. *Nat. Immunol.* 24, 267–279
- Guo, X. *et al.* (2018) Global characterization of T cells in non-small-cell lung cancer by single-cell sequencing. *Nat. Med.* 24, 978–985
- Moshofsky, K.B. *et al.* (2019) Acute myeloid leukemia-induced T-cell suppression can be reversed by inhibition of the MAPK pathway. *Blood Adv.* 3, 3038–3051
- Fu, Y. *et al.* (2023) Glycogen synthase kinase 3 controls T-cell exhaustion by regulating NFAT activation. *Cell. Mol. Immunol.* 20, 1127–1139
- Yan, S. *et al.* (2022) NKG2A and PD-L1 expression panel predicts clinical benefits from adjuvant chemotherapy and PD-L1 blockade in muscle-invasive bladder cancer. *J. Immunother. Cancer* 10, e004569
- Wang, Y. *et al.* (2022) Pilot study of a novel nanobody ⁶⁸Ga-NODAGA-SNA006 for instant PET imaging of CD8⁺ T cells. *Eur. J. Nucl. Med. Mol. Imaging* 49, 4394–4405
- Beckford Vera, D.R. *et al.* (2018) Immuno-PET imaging of tumor-infiltrating lymphocytes using zirconium-89 radiolabeled anti-CD3 antibody in immune-competent mice bearing syngeneic tumors. *PLoS One* 13, e0193832
- Pourmoori, N. *et al.* (2022) Magnetic resonance imaging of tumor-infiltrating lymphocytes by anti-CD3-conjugated iron oxide nanoparticles. *ChemMedChem* 17, e202100708
- Kist de Ruijter, L. *et al.* (2022) Whole-body CD8⁺ T cell visualization before and during cancer immunotherapy: a phase 1/2 trial. *Nat. Med.* 28, 2601–2610
- Farwell, M.D. *et al.* (2022) CD8-targeted PET imaging of tumor-infiltrating T cells in patients with cancer: a phase I first-in-humans study of ⁸⁹Zr-Df-IAB22M2C, a radiolabeled anti-CD8 minibody. *J. Nucl. Med.* 63, 720–726
- Wu, A.A. *et al.* (2015) Reprogramming the tumor microenvironment: tumor-induced immunosuppressive factors paralyze T cells. *Oncimmunology* 4, e1016700
- Rowe, S.P. and Pomper, M.G. (2022) Molecular imaging in oncology: current impact and future directions. *CA Cancer J. Clin.* 72, 333–352
- Kishton, R.J. *et al.* (2017) Metabolic regulation of T cell longevity and function in tumor immunotherapy. *Cell Metab.* 26, 94–109
- Akkaya, B. *et al.* (2018) Increased mitochondrial biogenesis and reactive oxygen species production accompany prolonged CD4⁺ T cell activation. *J. Immunol.* 201, 3294–3306
- Babin, V. *et al.* (2022) Late-stage carbon-14 labeling and isotope exchange: emerging opportunities and future challenges. *J. Am. Chem. Soc.* 144, 1234–1251
- Zaccagna, F. *et al.* (2018) Hyperpolarized carbon-13 magnetic resonance spectroscopic imaging: a clinical tool for studying tumour metabolism. *Br. J. Radiol.* 91, 20170688
- Choi, Y.S. *et al.* (2023) Hyperpolarized [¹⁻¹³C]pyruvate magnetic resonance spectroscopy shows that agmatine increased lactate production in the brain of type 2 diabetic mice. *Yonsei Med. J.* 64, 625–632
- Ardenkjaer-Larsen, J.H. *et al.* (2015) Facing and overcoming sensitivity challenges in biomolecular NMR spectroscopy. *Angew. Chem. Int. Ed. Engl.* 54, 9162–9185
- Stodkilde-Jorgensen, H. *et al.* (2020) Pilot study experiences with hyperpolarized [¹⁻¹³C]pyruvate MRI in pancreatic cancer patients. *J. Magn. Reson. Imaging* 51, 961–963
- Chen, H.Y. *et al.* (2020) Hyperpolarized ¹³C-pyruvate MRI detects real-time metabolic flux in prostate cancer metastases to bone and liver: a clinical feasibility study. *Prostate Cancer Prostatic Dis.* 23, 269–276
- Can, E. *et al.* (2020) Noninvasive rapid detection of metabolic adaptation in activated human T lymphocytes by hyperpolarized ¹³C magnetic resonance. *Sci. Rep.* 10, 200
- Kurhanewicz, J. *et al.* (2019) Hyperpolarized ¹³C MRI: path to clinical translation in oncology. *Neoplasia* 21, 1–16
- Gu, J. *et al.* (2021) DGK ζ exerts greater control than DGK α over CD8⁺ T cell activity and tumor inhibition. *Oncimmunology* 10, 1941566
- Radu, C.G. *et al.* (2008) Molecular imaging of lymphoid organs and immune activation by positron emission tomography with a new [¹⁸F]-labeled 2'-deoxycytidine analog. *Nat. Med.* 14, 783–788
- Lee, J.T. *et al.* (2012) Stratification of nucleoside analog chemotherapy using 1-(2'-deoxy-2'-¹⁸F-fluoro- β -D-arabinofuranosyl)cytosine and 1-(2'-deoxy-2'-¹⁸F-fluoro- β -L-arabinofuranosyl)-5-methylcytosine PET. *J. Nucl. Med.* 53, 275–280
- Schwarzenberg, J. *et al.* (2011) Human biodistribution and radiation dosimetry of novel PET probes targeting the deoxyribonucleoside salvage pathway. *Eur. J. Nucl. Med. Mol. Imaging* 38, 711–721
- Verri, A. *et al.* (1997) Relaxed enantioselectivity of human mitochondrial thymidine kinase and chemotherapeutic uses of L-nucleoside analogues. *Biochem. J.* 328, 317–320
- Kim, W. *et al.* (2016) [¹⁸F]CFA as a clinically translatable probe for PET imaging of deoxycytidine kinase activity. *Proc. Natl. Acad. Sci. U. S. A.* 113, 4027–4032
- Namavari, M. *et al.* (2011) Synthesis of 2'-deoxy-2'-[¹⁸F]fluoro-9- β -D-arabinofuranosylguanine: a novel agent for imaging T-cell activation with PET. *Mol. Imaging Biol.* 13, 812–818

How do we integrate different probes to achieve sensitive quantitative imaging of immune targets *in vivo*? It is challenging to establish dynamic changes in T cell activity *in vivo* with PET imaging. It might be more convenient to design sensitive 'off-on' imaging probes through protease activation, constituting a hot area of investigation.

How do we integrate imaging and the regulation of T cell activity *in vivo* using a single molecular probe? T-Fulips has set a successful example of -SH group modification; similar probes that center around different targets might need to be developed.

34. Antonios, J.P. *et al.* (2017) Detection of immune responses after immunotherapy in glioblastoma using PET and MRI. *Proc. Natl. Acad. Sci. U. S. A.* 114, 10220–10225
35. Levi, J. *et al.* (2019) Imaging of activated T cells as an early predictor of immune response to anti-PD-1 therapy. *Cancer Res.* 79, 3455–3465
36. Levi, J. *et al.* (2021) ¹⁸F-AraG PET for CD8 profiling of tumors and assessment of immunomodulation by chemotherapy. *J. Nucl. Med.* 62, 802–807
37. Tiwari, A. *et al.* (2022) Tumor microenvironment: barrier or opportunity towards effective cancer therapy. *J. Biomed. Sci.* 29, 83
38. Ni, K. *et al.* (2020) Nanoscale metal-organic frameworks generate reactive oxygen species for cancer therapy. *ACS Cent. Sci.* 6, 861–868
39. Gelderman, K.A. *et al.* (2006) T cell surface redox levels determine T cell reactivity and arthritis susceptibility. *Proc. Natl. Acad. Sci. U. S. A.* 103, 12831–12836
40. Chakraborty, P. *et al.* (2019) Thioredoxin-1 improves the immunometabolic phenotype of antitumor T cells. *J. Biol. Chem.* 294, 9198–9212
41. Messens, J. and Collet, J.F. (2013) Thiol-disulfide exchange in signaling: disulfide bonds as a switch. *Antioxid. Redox Signal.* 18, 1594–1596
42. Deng, H. *et al.* (2020) Targeted scavenging of extracellular ROS relieves suppressive immunogenic cell death. *Nat. Commun.* 11, 4951
43. Shi, C. *et al.* (2022) Targeting the activity of T cells by membrane surface redox regulation for cancer theranostics. *Nat. Nanotechnol.* 18, 86–97
44. Sena, L.A. *et al.* (2013) Mitochondria are required for antigen-specific T cell activation through reactive oxygen species signaling. *Immunity* 38, 225–236
45. Cui, D. *et al.* (2020) Semiconducting polymer nanoreporters for near-infrared chemiluminescence imaging of immunoactivation. *Adv. Mater.* 32, e1906314
46. Padgett, L.E. and Tse, H.M. (2016) NADPH oxidase-derived superoxide provides a third signal for CD4 T Cell effector responses. *J. Immunol.* 197, 1733–1742
47. Yi, M. *et al.* (2022) Combination strategies with PD-1/PD-L1 blockade: current advances and future directions. *Mol. Cancer* 21, 28
48. Natarajan, A. *et al.* (2015) Novel radiotracer for immunoPET imaging of PD-1 checkpoint expression on tumor infiltrating lymphocytes. *Bioconjug. Chem.* 26, 2062–2069
49. Du, Y. *et al.* (2017) Nuclear and fluorescent labeled PD-1-Liposome-DOX-⁶⁴Cu/IRDye800CW allows improved breast tumor targeted imaging and therapy. *Mol. Pharm.* 14, 3978–3986
50. England, C.G. *et al.* (2018) ⁸⁹Zr-labeled nivolumab for imaging of T-cell infiltration in a humanized murine model of lung cancer. *Eur. J. Nucl. Med. Mol. Imaging* 45, 110–120
51. Niemeijer, A. *et al.* (2018) Whole body PD-1 and PD-L1 positron emission tomography in patients with non-small-cell lung cancer. *Nat. Commun.* 9, 4664
52. Kok, I. *et al.* (2022) ⁸⁹Zr-pembrolizumab imaging as a non-invasive approach to assess clinical response to PD-1 blockade in cancer. *Ann. Oncol.* 33, 80–88
53. Zhang, H. *et al.* (2021) A chimeric antigen receptor with antigen-independent OX40 signaling mediates potent antitumor activity. *Sci. Transl. Med.* 13, eaba7308
54. Chen, X. *et al.* (2019) Early therapeutic vaccination prediction of hepatocellular carcinoma via imaging OX40-mediated tumor infiltrating lymphocytes. *Mol. Pharm.* 16, 4252–4259
55. Alam, I.S. *et al.* (2018) Imaging activated T cells predicts response to cancer vaccines. *J. Clin. Invest.* 128, 2569–2580
56. Alam, I.S. *et al.* (2020) Visualization of activated T Cells by OX40-immunoPET as a strategy for diagnosis of acute graft-versus-host disease. *Cancer Res.* 80, 4780–4790
57. Rujas, E. *et al.* (2020) Structural characterization of the ICOS/ICOS-L immune complex reveals high molecular mimicry by therapeutic antibodies. *Nat. Commun.* 11, 5066
58. Simonetta, F. *et al.* (2021) Molecular imaging of chimeric antigen receptor T cells by ICOS-immunoPET. *Clin. Cancer Res.* 27, 1058–1068
59. Xiao, Z. *et al.* (2020) ICOS is an indicator of T-cell-mediated response to cancer immunotherapy. *Cancer Res.* 80, 3023–3032
60. Persson, J. *et al.* (2021) Discovery, optimization and biodistribution of an Affibody molecule for imaging of CD69. *Sci. Rep.* 11, 19151
61. Edwards, K.J. *et al.* (2022) Using CD69 PET imaging to monitor immunotherapy-induced immune activation. *Cancer Immunol. Res.* 10, 1084–1094
62. Nisnboym, M. *et al.* (2023) Immuno-PET imaging of CD69 visualizes T-cell activation and predicts survival following immunotherapy in murine glioblastoma. *Cancer Res. Commun.* 3, 1173–1188
63. Wang, X. *et al.* (2022) Preclinical and exploratory human studies of novel (68)Ga-labeled D-peptide antagonist for PET imaging of TIGIT expression in cancers. *Eur. J. Nucl. Med. Mol. Imaging* 49, 2584–2594
64. Wei, W. *et al.* (2020) ImmunoPET imaging of TIM-3 in murine melanoma models. *Adv. Ther. (Weinh)* 3, 2000018
65. Lecocq, Q. *et al.* (2020) The next-generation immune checkpoint LAG-3 and its therapeutic potential in oncology: third time's a charm. *Int. J. Mol. Sci.* 22, 75
66. Kelly, M.P. *et al.* (2018) Immuno-PET detection of LAG-3 expressing intratumoral lymphocytes using the zirconium-89 radiolabeled fully human anti-LAG-3 antibody REGN3767. *Cancer Res.* 78, 3033
67. Miedema, I.H.C. *et al.* (2023) ⁸⁹Zr-immuno-PET using the anti-LAG-3 tracer [⁸⁹Zr]Zr-BI 754111: demonstrating target specific binding in NSCLC and HNSCC. *Eur. J. Nucl. Med. Mol. Imaging* 50, 2068–2080
68. Larimer, B.M. *et al.* (2017) Granzyme B PET imaging as a predictive biomarker of immunotherapy response. *Cancer Res.* 77, 2318–2327
69. Nguyen, A. *et al.* (2020) Granzyme B nanoreporter for early monitoring of tumor response to immunotherapy. *Sci. Adv.* 6, eabc2777
70. Mac, Q.D. *et al.* (2019) Non-invasive early detection of acute transplant rejection via nanosensors of granzyme B activity. *Nat. Biomed. Eng.* 3, 281–291
71. He, S. *et al.* (2023) Activatable near-infrared probes for the detection of specific populations of tumour-infiltrating leukocytes in vivo and in urine. *Nat. Biomed. Eng.* 7, 1–17
72. Zhao, N. *et al.* (2021) In vivo measurement of granzyme proteolysis from activated immune cells with PET. *ACS Cent. Sci.* 7, 1638–1649
73. Garnier, L. *et al.* (2022) IFN-γ dependent tumor-antigen cross-presentation by lymphatic endothelial cells promotes their killing by T cells and inhibits metastasis. *Sci. Adv.* 8, eabl5162
74. Gibson, H.M. *et al.* (2018) IFN-γ PET Imaging as a predictive tool for monitoring response to tumor immunotherapy. *Cancer Res.* 78, 5706–5717
75. Rezazadeh, F. *et al.* (2022) Evaluation and selection of a lead diabody for interferon-gamma PET imaging. *Nucl. Med. Biol.* 114–115, 162–167
76. Hsu, E.J. *et al.* (2021) A cytokine receptor-masked IL-2 prodrug selectively activates tumor-infiltrating lymphocytes for potent antitumor therapy. *Nat. Commun.* 12, 2768
77. Ross, S.H. and Cantrell, D.A. (2018) Signaling and function of interleukin-2 in T lymphocytes. *Annu. Rev. Immunol.* 36, 411–433
78. Di Gialleonardo, V. *et al.* (2012) N-(4-¹⁸F-fluorobenzoyl)interleukin-2 for PET of human-activated T lymphocytes. *J. Nucl. Med.* 53, 679–686
79. Hartimath, S.V. *et al.* (2017) Noninvasive monitoring of cancer therapy induced activated T cells using [¹⁸F]FB-IL-2 PET imaging. *Oncimmunology* 6, e1248014
80. van de Donk, P.P. *et al.* (2021) Interleukin-2 PET imaging in patients with metastatic melanoma before and during immune checkpoint inhibitor therapy. *Eur. J. Nucl. Med. Mol. Imaging* 48, 4369–4376
81. Markovic, S.N. *et al.* (2018) Non-invasive visualization of tumor infiltrating lymphocytes in patients with metastatic melanoma undergoing immune checkpoint inhibitor therapy: a pilot study. *Oncotarget* 9, 30268–30278
82. van der Veen, E.L. *et al.* (2020) Development and evaluation of interleukin-2-derived radiotracers for PET imaging of T cells in mice. *J. Nucl. Med.* 61, 1355–1360

83. Zhang, X. *et al.* (2021) Bioengineering tools for probing intracellular events in T lymphocytes. *WIREs Mech. Dis.* 13, e1510
84. Samimi, K. *et al.* (2021) Time-domain single photon-excited autofluorescence lifetime for label-free detection of T cell activation. *Opt. Lett.* 46, 2168–2171
85. Gohring, J. *et al.* (2021) Temporal analysis of T-cell receptor-imposed forces via quantitative single molecule FRET measurements. *Nat. Commun.* 12, 2502
86. Pielak, R.M. *et al.* (2017) Early T cell receptor signals globally modulate ligand:receptor affinities during antigen discrimination. *Proc. Natl. Acad. Sci. U. S. A.* 114, 12190–12195
87. Wu, J. *et al.* (2021) Asparagine enhances LCK signalling to potentiate CD8⁺ T-cell activation and anti-tumour responses. *Nat. Cell Biol.* 23, 75–86
88. Dustin, M.L. (2003) Coordination of T cell activation and migration through formation of the immunological synapse. *Ann. N. Y. Acad. Sci.* 987, 51–59
89. Boczek, T. *et al.* (2017) Cross talk among PMCA, calcineurin and NFAT transcription factors in control of calmodulin gene expression in differentiating PC12 cells. *Biochim. Biophys. Acta Gene Regul. Mech.* 1860, 502–515
90. Grakoui, A. *et al.* (2002) The immunological synapse: a molecular machine controlling T cell activation. *Science* 285, 221–227
91. Dustin, M.L. and Depoil, D. (2011) New insights into the T cell synapse from single molecule techniques. *Nat. Rev. Immunol.* 11, 672–684
92. Lodygin, D. and Flugel, A. (2017) Intravital real-time analysis of T-cell activation in health and disease. *Cell Calcium* 64, 118–129
93. Yi, J. *et al.* (2019) TCR microclusters form spatially segregated domains and sequentially assemble in calcium-dependent kinetic steps. *Nat. Commun.* 10, 277
94. Capera, J. *et al.* (2023) Dynamics and spatial organization of Kv1.3 at the immunological synapse of human CD4⁺ T cells. *Biophys. J.* Published online August 18, 2023. <https://doi.org/10.1016/j.bpj.2023.08.011>
95. Kvalvaag, A. *et al.* (2023) Clathrin mediates both internalization and vesicular release of triggered T cell receptor at the immunological synapse. *Proc. Natl. Acad. Sci. U. S. A.* 120, e2211368120
96. Velas, L. *et al.* (2021) Three-dimensional single molecule localization microscopy reveals the topography of the immunological synapse at isotropic precision below 15 nm. *Nano Lett.* 21, 9247–9255
97. Dustin, M.L. (2021) Tireless surveillance by exhausted T cells. *J. Clin. Invest.* 131, e144353
98. Friedman, R.S. *et al.* (2010) Real-time analysis of T cell receptors in naive cells in vitro and in vivo reveals flexibility in synapse and signaling dynamics. *J. Exp. Med.* 207, 2733–2749
99. Marangoni, F. *et al.* (2013) The transcription factor NFAT exhibits signal memory during serial T cell interactions with antigen-presenting cells. *Immunity* 38, 237–249
100. Huppa, J.B. *et al.* (2010) TCR-peptide-MHC interactions in situ show accelerated kinetics and increased affinity. *Nature* 463, 963–967
101. Ma, Y. *et al.* (2017) An intermolecular FRET sensor detects the dynamics of T cell receptor clustering. *Nat. Commun.* 8, 15100
102. Yudushkin, I.A. and Vale, R.D. (2010) Imaging T-cell receptor activation reveals accumulation of tyrosine-phosphorylated CD3 ζ in the endosomal compartment. *Proc. Natl. Acad. Sci. U. S. A.* 107, 22128–22133
103. Wan, R. *et al.* (2019) Biophysical basis underlying dynamic Lck activation visualized by ZapLck FRET biosensor. *Sci. Adv.* 5, eaau2001
104. Ouyang, M. *et al.* (2019) Sensitive FRET biosensor reveals Fyn kinase regulation by submembrane localization. *ACS Sens.* 4, 76–86